

## Surface Anchoring and Growth Pattern of the Field-Driven First-Order Transition in a Smectic-A Liquid Crystal

Zili Li \*

Liquid Crystal Institute, Kent State University, Kent, Ohio 44242

Oleg D. Lavrentovich†

Liquid Crystal Institute and Department of Physics, Kent State University, Kent, Ohio 44242

(Received 21 May 1993; revised manuscript received 11 April 1994)

It is demonstrated that a surface energy anisotropy (anchoring) defines the growth pattern of the field-induced transition in a smectic-A liquid crystal (Sm-A). The stable domain phase nucleates as rounded domains but expands as stripes. The change in growth pattern is accounted for a large anchoring strength  $W_a \sim 10^{-2} - 10^{-3} \text{ J/m}^2$  which is connected with the layer breaking in the vicinity of the cell plates. The temperature dependence of  $W_a$  for Sm-A (substance CCN-47) is measured for the first time:  $W_a \sim (T_{A-N} - T)^{0.65 \pm 0.09}$ .

PACS numbers: 64.70.Md, 61.30.-v, 61.50.Cj

The propagation of fronts separating stable and unstable states and resulting growth patterns form an interesting class of physical problems [1]. A principal question is a variation of the growth patterns in systems with anisotropy [1-4]. The anisotropy can be external (liquid/gas front propagating in a Hele-Shaw cell with engraved plates) or intrinsic (gas propagating in a cell filled with liquid crystal, solidification). Systems with intrinsic anisotropy such as liquid crystals are especially important to study the relation between global pattern asymmetry and local (molecular) asymmetry. In the situations studied (see, e.g., Refs. [2,3]), molecular asymmetry manifested itself in the anisotropy of viscosity, i.e., as a *bulk effect*. However, the intrinsic anisotropy can show up also in *surface properties*. Molecular interactions at the interface between a liquid crystal and an ambient medium establish a definite orientation  $\mathbf{n}_0$  of the director  $\mathbf{n}$ . The deviations of  $\mathbf{n}$  from  $\mathbf{n}_0$  require some energy; this phenomenon is known as surface anchoring [4].

We report results of experiments on field-driven first-order transition in a Sm-A demonstrating the effect of *surface anchoring* on growth patterns. The anchoring coefficient  $W_a$  and its temperature dependence in the Sm-A phase are measured for the first time. The results show a principal difference in anchoring of the Sm-A phase which presents bulk one-dimensional positional order and a nematic (N) phase which possesses only orientational order. The difference manifests itself in surprisingly large  $W_a$  in the Sm-A phase and is accounted for by a layered structure of Sm-A.

Sm-A consists of rodlike molecules that form parallel liquid layers to which the molecules are normal. Thin (10-100  $\mu\text{m}$ ) flat cells were filled with Sm-A layers parallel to the cell plates. The plates were coated with indium-tin-oxide electrodes and treated by a 0.1% lecithin solution to achieve a homeotropic orientation. The cell thickness  $h$  was measured by the interference technique with an accuracy of 2%. Liquid

crystal CCN-47 (4'-trans-butyl-4-cyano-4-trans-heptyl-1, 1'-bicyclohexane) purchased from E.M. Industries ( $C \xrightarrow{<10^\circ\text{C}} \text{Sm-A} \xrightarrow{30.7 \pm 0.3} N$ ) was investigated. The relative dielectric anisotropy  $\epsilon_a = \epsilon_{\parallel} - \epsilon_{\perp}$  is negative (the subscripts refer to  $\mathbf{n}$  which is the layer normal). By measuring the capacitance of homogeneous and homeotropic cells, we obtained  $\epsilon_{\parallel}$  and  $\epsilon_{\perp}$ ; in the Sm-A phase  $\epsilon_a$  changes slowly from (-9.1) at 30 °C to (-10.8) at 15 °C. Temperature control was better than 25 mK; the temperature gradients across the  $1 \times 2 \text{ cm}^2$  cell were smaller than 50 mK/mm. A vertical ac (1.5 kHz) electric field  $\mathbf{E}$  was applied to the cell electrodes. Since  $\epsilon_a < 0$ , a sufficiently strong field is expected to reorient the Sm-A layers. The voltage increase rate was very slow, typically  $1 \times 10^{-2} \text{ V/sec}$  near the threshold.

At small voltages,  $U = Eh$ , the initial structure remains homeotropic:  $\mathbf{n}$  is oriented vertically and the structure is black under the polarizing microscope. As  $U$  increases, in some particular sites the optical axis  $\mathbf{n}$  reorients and circular bright spots appear [Fig. 1(a)]; they grow up with  $U$  [Fig. 1(b)]. The horizontal projection  $\mathbf{n}_{xy}$  of  $\mathbf{n}$  is axially symmetric, indicating that the spots represent small torical focal domains (TD) [5] [Fig. 2(a)]. The voltage of TD nucleation is different for different sites; i.e., the nucleation is a heterogeneous process, facilitated by bulk or surface imperfections [6]. It is confirmed also by the following observations: The initial homeotropic state can be restored by removal of field and heating; in the new cycle of the field increase TDs appear at the same sites.

When the diameter  $2a$  of the TD reaches some critical value close to the cell thickness  $h$ , the growth pattern changes. The stable phase starts to propagate via stripe domains (SD) emerging from the TDs rather than by the increase of  $a$  [Fig. 1(c)]. The elongation of SD has a well-defined threshold  $U_{SD}$  that is the same for the sites where the TDs were initially created;  $U_{SD}$  is reproducible for different samples of the same thickness. For  $U \approx U_{SD}$

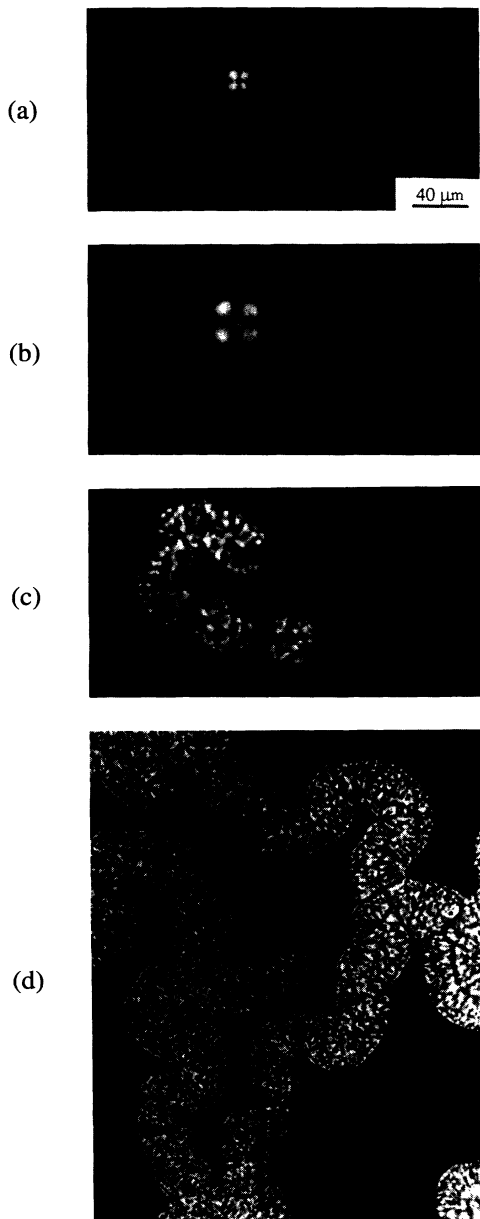


FIG. 1. Growth of the field-deformed phase in the Sm-A homeotropic cell with thickness  $h = 37 \mu\text{m}$ : (a) nucleation and (b) growth of the TD,  $U < U_{SD}$ ; appearance (c) and elongation (d) of the SDs,  $U = U_{SD}$ .

the SD slowly ( $< 1 \mu\text{m}/\text{min}$ ) elongates keeping a constant width  $2a \approx h$  [Fig. 1(d)].

There are several important features of SD texture: (a) An averaged  $\mathbf{n}_{xy}$  is normal to the SD symmetry plane; (b) the ends of the SD are represented by semicircular TDs; and (c) the layer tilt increases as one moves from the edge of the SD to the central vertical plane. These peculiarities allow us to associate the SDs with well-known oily streaks [5, 7] that have a basic structure represented by Fig. 2(b). The threshold  $U_{SD}$  depends on

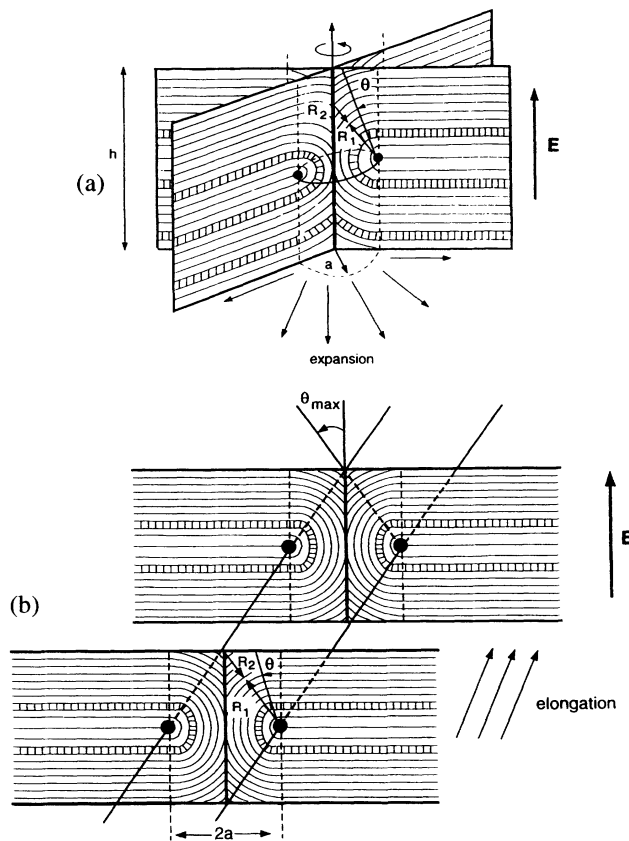


FIG. 2. Structure of the TD (a) and SD (b). Arrows show the horizontal direction of expansion when the external vertical field increases. The wall defect of the SD is most probably replaced by a set of focal conics (not shown) which provides the striation of the SD visible in Figs. 1(c) and 1(d).

the cell thickness  $U_{SD} \sim \sqrt{h}$ ; see Fig. 3. We also investigated the temperature dependence  $U_{SD}(T)$ ; see Fig. 4. Several experimental runs give the same result:  $U_{SD}(T)$  shows a power law dependence,  $U_{SD} \sim (\Delta T)^\alpha$ , where  $\Delta T = T_{A-N} - T$ ,  $\alpha$  and  $T_{A-N}$  are constants. The value  $T_{A-N}$  was first chosen at the point where  $|dU_{SD}/dT|$  is maximal; it agrees with the temperature of the Sm-A-N transition defined under the microscope. Then we took into account finite temperature steps in the experimental data and  $T_{A-N}$  was varied by the  $0.025^\circ\text{C}$  steps. A single power law was obeyed for all cases over 2.5 decades in  $\Delta T/T$  and for  $T_{A-N}$  in the range of  $30.70^\circ\text{C}$ - $30.60^\circ\text{C}$ . In this way a set of exponents  $\alpha$  was obtained using the linear least-squares fit and the resulting  $\alpha = 0.32 \pm 0.03$  was taken as the average value.

The observed transition has a pronounced first-order character; it is confirmed, e.g., by a sharp interface between the domain and homeotropic phases (see [8] and discussion below). In fact, field-induced transitions have been detected in Sm-A with  $\epsilon_a < 0$  [9]; however, the scenario of the process has not been reported. The nucleation of TDs was observed for the lyotropic Sm-A mixed with ferrofluid [10]. To explain the growth pattern

let us consider the energy and geometry of the Sm-A domain defects.

The free energy of the deformed Sm-A volume  $V$  bounded by the surface  $S$  is composed by energy of

$$F = F_K + F_B + F_E + F_W + F_{\text{core}} = \frac{1}{2} \int_V [K(R_1^{-1} + R_2^{-1})^2 + B\delta^2 - \epsilon_0 \epsilon_a (\mathbf{n} \cdot \mathbf{E})^2] dv + \int_S W(\theta) ds + F_{\text{core}}, \quad (1)$$

where  $K$  is a curvature modulus,  $R_1$  and  $R_2$  are principal radii of layer curvature,  $B$  is a compression modulus that describes the elastic resistance to changes  $\delta$  in the layer thickness  $d$ ,  $\epsilon_0$  is the dielectric constant of vacuum, and  $W$  is an angular-dependent part of surface free energy.

Inside a TD, the layers with saddlelike curvature fold around a circle; this circle as well as the line of rotation symmetry are two linear defects. The radii  $R_1$  and  $R_2$  are centered at the circle and the rotation axis, respectively. In the central part the layers are oriented vertically [Fig. 2(a)].

The stripe domain is a stripe analog of TD: Horizontal curvature  $R_2^{-1} = 0$ . The symmetry axis transforms into the plane and the circle transforms into two horizontal lines [Fig. 2(b)]. Both TD and SD keep  $\delta = 0$  everywhere except at two lines (TD) or at two lines and a central wall defect (SD). Thus  $F_B = 0$  and the energy losses connected with the layer breaking at the core of defects and, perhaps, at the surface of the cell, can be included into  $F_{\text{core}}$  and  $F_W$ .

As was shown by Bidaux *et al.* [11], the most suitable geometry of the wall defect is a set of focal conics with energy  $F_{\text{core}} \cong K(h/\lambda)^{1/3}$ , where  $\lambda = \sqrt{K/B}$  is of the order of  $d$  in the deep Sm-A phase. These focal conics are not shown in Fig. 2(b), but some of them are visible in the textures of SD. Because of  $F_{\text{core}}$  the elastic cost of the SD propagation is *higher* than that of the TD expansion: All other elastic terms associated with the curvature of layers in both SD and TD or

pure curvatures  $F_K$ , dilation energy  $F_B$ , energy of cores of singularities  $F_{\text{core}}$ , dielectric energy  $F_E$ , and surface energy  $F_W$  [5]:

with line singularities in TD,  $F_K \cong K$  (per unit length), can be neglected,  $F_K/F_{\text{core}} \sim (\lambda/h)^{1/3} \ll 1$ . We have to conclude that *the elastic energy does not favor the TD-SD transformation.*

The SD appearance becomes even more puzzling when one considers the gain in the dielectric energy  $F_E < 0$  that is brought about by the layer reorientation and is the only source of the structural instabilities. As is easy to see from Eq. (1) *the gain in the dielectric energy for SD is smaller than that for the TD.* Really,  $|F_E|$  grows with reorientation angle  $\theta$  between  $\mathbf{n}$  and  $\mathbf{E}$ ,  $\cos\theta = (\mathbf{n} \cdot \mathbf{E})$ . The maximal  $\theta$  is defined by the TD diameter or SD width:  $\theta_{\text{max}} = \arctan(2a/h)$ . Therefore the increase in  $a$  results in the increase of  $\theta_{\text{max}}$  (Fig. 2) and in the increase of  $|F_E|$ . For the expanding TD  $\theta_{\text{max}} \rightarrow \pi/2$  and  $|F_E|$  reaches the maximum  $|F_E(\theta_{\text{max}} = \pi/2)|$ . For the SD  $\theta_{\text{max}}$  remains *fixed* by the constant width of SD and is always smaller than  $\pi/2$ :  $\theta_{\text{max}} \approx \pi/4$  for  $2a \approx h$  [Fig. 2(b)]. *Thus the dielectric energy does not favor the TD-SD transformation either.*

There is only one remaining term in Eq. (1) able to favor the SD vs TD. This is the anchoring  $F_W$  defined as the work one needs to spend to reorient the molecules from  $\theta = 0$  to  $\theta \neq 0$ . The expansion of the TD means that the layers reorient normally,  $\theta_{\text{max}} \rightarrow \pi/2$ . In

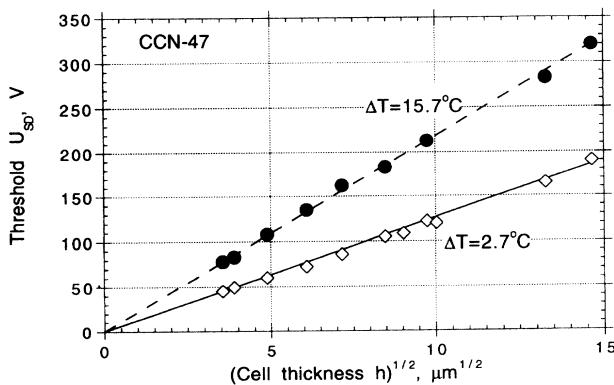


FIG. 3. Threshold voltage of the stripe domain elongation  $U_{SD}$  vs  $\sqrt{h}$  for two temperatures  $\Delta T = 15.7^\circ\text{C}$  and  $\Delta T = 2.7^\circ\text{C}$ : experimental data (circles and diamonds, respectively; the error is smaller than the symbol size) and theoretical curves calculated from Eq. (2) with  $W_a = 11.4 \times 10^{-3} \text{ J/m}^2$  and  $W_a = 3.4 \times 10^{-3} \text{ J/m}^2$ , respectively.

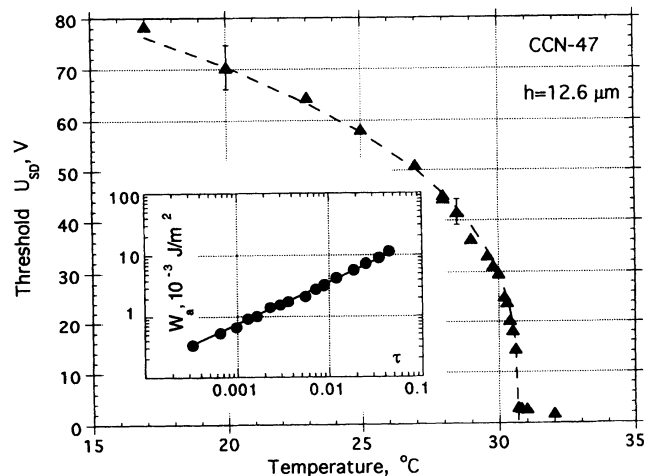


FIG. 4. Threshold voltage of the stripe domain elongation  $U_{SD}$  vs temperature  $T$  for  $12.6 \mu\text{m}$  sample,  $U_{SD} \sim (T_{A-N} - T)^{0.32 \pm 0.03}$ ; the line is the fit  $U_{SD} = U_{SD,0} \tau^{0.32}$ , where  $\tau = (T_{A-N} - T)/T_{A-N}$ ,  $U_{SD} = 205.4 \text{ V}$ , and  $T_{A-N} = 303.86 \text{ K}$ . The inset is the log-log plot  $W_a(\tau)$ ; the slope gives  $W_a \sim \tau^{0.65 \pm 0.09}$ ; a typical fit  $W_a = W_{a,0} \tau^{0.69}$  with  $W_{a,0} = 0.09 \text{ J/m}^2$  is shown by the line.

contrast, the expansion of SD via elongation *does not require complete reorientation*. As SD elongates, maximal surface tilt  $\theta_{\max} \approx \pi/4$  remains fixed and smaller than  $\pi/2$ ; Fig. 2(b). Thus the change in the growth pattern can be explained by the fact that the *anchoring cost of the SD elongation is smaller than that of the TD expansion*.

Let us proceed to the calculation of the threshold  $U_{SD}$  defined by  $F_{\text{core}}$ ,  $F_E$ , and  $F_W$ . The contribution  $F_{\text{core}} \cong K(h/\lambda)^{1/3}$  per unit length of the SD follows from Ref. [11]. An integration of the field term in Eq. (1) over the vertical cross section of SD gives the energy gain:  $F_E = \varepsilon_0 \varepsilon_a E^2 h^2 / 4$ . The calculation of  $F_W$  is more difficult.

To define  $F_W$ , one ideally needs to know the analytical expression for  $W(\theta)$ . Unfortunately,  $W(\theta)$  for Sm-A placed on a plate coated by surfactant molecules is unknown. Usually for  $N$  one has monotonous function  $W(\theta) \sim \sin^2 \theta$ . Sm-A can differ in anchoring properties from  $N$  because of layered structure. Any tilted orientation requires a breaking of the layers to fill the space in the vicinity of a plate. If the plate is absolutely flat, there are only two extreme orientations where the layers can fill the space smoothly,  $\theta = 0$  and  $\theta = \pi/2$ . Therefore  $W(\theta)$  can be nonmonotonous with two minima at  $\theta = 0, \pi/2$  and a maximum between them. To avoid an unnecessary oversimplification, we will operate with the integral representation,  $F_W = W_a h$ , where the anchoring strength is  $W_a = 4 \int_0^{a/h} W[\theta(x)] dx$ ,  $x$  is the dimensionless transversal horizontal coordinate, and factor 4 is determined by the SD symmetry.

The condition of zero line tension of the SD,  $F_{\text{core}} + F_E + F_W = 0$ , defines  $U_{SD}$ :

$$U_{SD}^2 = 4(\varepsilon_0 |\varepsilon_a|)^{-1} h (W_a + Kh^{-2/3} \lambda^{-1/3}). \quad (2)$$

Since the experiment shows  $U_{SD} \sim h^{1/2}$ , one concludes that *the anchoring  $W_a$  is the main factor that defines  $U_{SD}$* . Quantitative analysis confirms this conclusion. The slope  $U_{SD}(\sqrt{h})$  (Fig. 3) gives an estimate of the total energy cost of the SD propagation; for different  $T$ ,  $W_a + Kh^{-2/3} \lambda^{-1/3} \approx 10^{-3} - 10^{-2} \text{ J/m}^2$ . With typical  $K = 10^{-11} \text{ N}$ ,  $h = 30 \mu\text{m}$ ,  $\lambda = 30 \text{ \AA}$ , one has  $Kh^{-2/3} \lambda^{-1/3} \approx 10^{-5} \text{ J/m}^2$ , i.e.,  $Kh^{-2/3} \lambda^{-1/3} \ll W_a$ . Therefore,  $U_{SD}$  is defined by  $W_a$  rather than by the elastic term. Two lines in Fig. 3 represent  $U_{SD}(\sqrt{h})$  calculated from Eq. (2) using  $K$  and  $\lambda$  as above and measured  $|\varepsilon_a|$  (10.8 and 9.5, respectively). The only free parameter is  $W_a$ . With  $W_a = 11.4 \times 10^{-3} \text{ J/m}^2$  at  $\Delta T = 15.7^\circ \text{C}$  and  $W_a = 3.4 \times 10^{-3} \text{ J/m}^2$  at  $\Delta T = 2.7^\circ \text{C}$  the agreement between the experimental and theoretical data is good.

Equation (2) allows us to find  $W_a(T)$  using  $U_{SD}(T)$  and  $\varepsilon_a(T)$  data. One gets  $W_a \sim (\Delta T)^{0.65 \pm 0.09}$ , and  $W_a$  in the range  $10^{-3} - 10^{-2} \text{ J/m}^2$ ; see the inset in Fig. 4. Thus at the Sm-A lecithin coated rigid plate  $W_a$  is significantly higher than  $W_a \sim 10^{-7} - 10^{-3} \text{ J/m}^2$  measured for  $N$  [4] and than the anisotropy of the surface energy  $\Delta W = W(\theta = \pi/2) - W(\theta = 0) \sim 10^{-7} - 10^{-5} \text{ J/m}^2$  found for a Sm-A liquid interface [12].

The energy  $F_l$  per unit surface needed to destroy the layered structure can be roughly estimated as  $Bd$ . With  $B \sim 10^5 - 10^7 \text{ J/m}^3$ ,  $d \sim 30 \text{ \AA}$  one has  $F_l \sim (0.3 - 30) \times 10^{-3} \text{ J/m}^2$ . Therefore it is likely that our findings reflect the fact that  $W_a \sim F_l \sim Bd$ . Similar estimations follow from models proposed by Durand [13]. Dependence  $W_a \sim (\Delta T)^{0.65 \pm 0.09}$  also indicates that  $W_a$  has temperature behavior similar to that of  $B$  [14]. Qualitatively, it means that the anchoring phenomena in Sm-A are defined not only by the anisotropic interaction liquid crystal substrate but also by the very nature of the layered Sm-A structure: The tilt requires a breaking of layers. In the nematic phase the layers do not exist and  $W_a$  can be smaller; however, if the boundary introduces the smecticlike surface ordering [4],  $W_a$  can also be high for the  $N$  phase.

Similar TD-SD transformations in growth patterns can occur in other systems; preliminary experiments [15] for cholesteric, Sm-C, and lyotropic phases indicate this possibility.

We are grateful to D.L. Johnson, M. Kléman, P. Palfy-Muhoray, V.M. Pergamenschchik, and Ch. Rosenblatt for valuable discussions. This work was supported by NSF Grant No. DMR89-20147 and by DARPA Contract No. MDA972-90-C-0037.

\*Present address: Science Center, Rockwell International Corp., Thousand Oaks, CA 91358.

†Also at Institute of Physics, Academy of Sciences, Kyiv, Ukraine.

- [1] D. A. Kessler, J. Koplik, and H. Levine, *Adv. Phys.* **37**, 255 (1988).
- [2] A. Buka, J. Kertész, and T. Vicsek, *Nature (London)* **323**, 424 (1986).
- [3] A. Buka and P. Palfy-Muhoray, *J. Phys. (Paris)* **49**, 1319 (1988).
- [4] B. Jérôme, *Rep. Prog. Phys.* **54**, 391 (1991).
- [5] M. Kléman, *Points, Lines and Walls in Liquid Crystals, Magnetic Systems and Various Ordered Media* (Wiley, New York, 1983).
- [6] O. D. Lavrentovich and M. Kléman, *Phys. Rev. E* **48**, 39 (1993); O. D. Lavrentovich, M. Kléman, and V. M. Pergamenschchik, *J. Phys. II (France)* **4**, 377 (1994).
- [7] S. A. Asher and P. S. Pershan, *Biophys. J.* **27**, 393 (1979).
- [8] P. E. Cladis *et al.*, *Phys. Rev. Lett.* **62**, 1764 (1989).
- [9] M. Goscianski, L. Leger, and A. Mircea-Roussel, *J. Phys. (Paris), Lett.* **36**, L-313 (1975).
- [10] J. C. Dabadie *et al.*, *J. Phys. Condens. Matter* **2**, SA291 (1990).
- [11] R. Bidaux *et al.*, *J. Phys. (Paris)* **34**, 661 (1973).
- [12] O. D. Lavrentovich, *Zh. Eksp. Teor. Fiz.* **91**, 1666 (1986) [*Sov. Phys. JETP* **64**, 984 (1986)]; *Mol. Cryst. Liq. Cryst.* **151**, 417 (1987).
- [13] G. Durand, *Liq. Cryst.* **14**, 159 (1993).
- [14] T. C. Lubensky, *J. Chim. Phys.* **80**, 31 (1983).
- [15] P. Fabre *et al.*, (private communication).

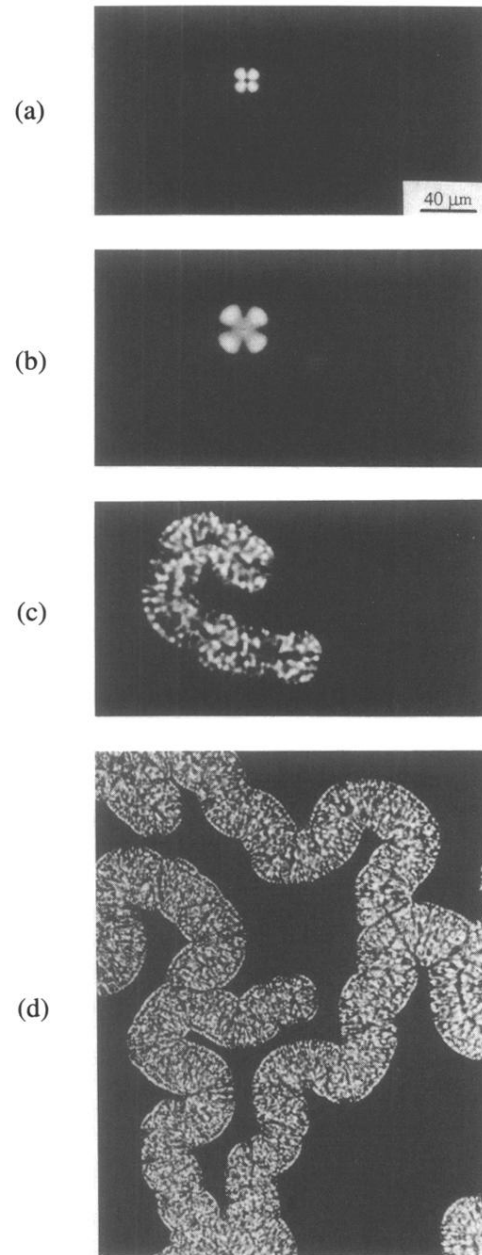


FIG. 1. Growth of the field-deformed phase in the Sm-A homeotropic cell with thickness  $h = 37 \mu\text{m}$ : (a) nucleation and (b) growth of the TD,  $U < U_{\text{SD}}$ ; appearance (c) and elongation (d) of the SDs,  $U = U_{\text{SD}}$ .